2023-08-01

X-Ray Crystal Structure Of E399q,e708q Ecm16 Double Mutant

Gileydis Guillama
University of Texas at El Paso

X-RAY CRYSTAL STRUCTURE OF E399Q,E708Q ECM16 DOUBLE MUTANT

GILEYDIS GUILLAMA BARROSO

Master's Program in Chemistry

APPROVED:

Chu-Young Kim, Ph.D., Chair

Mahesh Narayan, Ph.D.

Priyanka Gade, Ph.D.

Stephen L. Crites, Jr., Ph.D.
Dean of the Graduate School

X-RAY CRYSTAL STRUCTURE OF E399Q,E708Q ECM16 DOUBLE MUTANT.

by

B.S. GILEYDIS GUILLAMA BARROSO

THESIS

Presented to the Faculty of the Graduate School of

The University of Texas at El Paso

in Partial Fulfillment

of the Requirements

for the Degree of

MASTER OF SCIENCE

Department of Chemistry and Biochemistry

THE UNIVERSITY OF TEXAS AT EL PASO, TX

August 2023

Abstract

The use of antibiotics has undoubtedly been a boon for humanity in combating infections and microbial threats. However, their widespread utilization has contributed to the emergence and spread of antibiotic resistance, which now poses a significant public health challenge. *Streptomyces* bacterium, produce diverse secondary metabolites with antibacterial, antifungal, antiviral, antitumoral, and immunosuppressant activities. Among these compounds is echinomycin, a nonribosomal peptide antibiotic synthesized by *Streptomyces lasalocidi*, which inhibits DNA replication and transcription by intercalating the DNA duplex at CpG steps. A gene called ecm16 was identified in the echinomycin biosynthetic gene cluster, which provides echinomycin self-resistance. Ecm16 recognizes DNA duplexes that contain echinomycin, and neutralizes its toxicity through a yet undetermined mechanism. To shed light on this process, we are determining the crystal structure of Ecm16 containing ATP. We introduced strategic mutations in the nucleotide binding site of Ecm16 to prevent ATP hydrolysis. We have successfully cloned, expressed, and purified the recombinant Ecm16 E399Q,E708Q double mutant protein. We have solved the structure of this protein using X-ray Crystallography at a resolution of 2.07 Å. However, our crystal structure contained ADP instead of the expected ATP. We propose and alternative experimental strategies for structure determination of ATP-containing Ecm16.

Acknowledgement

I extend my heartfelt gratitude to my advisor, Dr. Chu-Young Kim, for his support and guidance throughout my master's journey. His constant motivation has been instrumental in keeping me focused and determined. I would like to express my appreciation to my Research Advisor Committee members, Dr. Mahesh Narayan, and Dr. Priyanka Gade, for their valuable advice and encouragement during this time. Their insights have played a significant role in advancing my work. A special thanks goes to Dr. Irimpam Mathews for his assistance in data collection at SSRL and for providing valuable input that has contributed to the progress of my research.

I am grateful to my fellow lab members, Dr. Anwar, Dr. Manas, B.S. Gerardo, M.S. Dayan and B.S. Payam, for making my lab experience more enjoyable and for their support. Our scientific and non-scientific discussions and the fun moments will be cherished. I would also like to thank my friends at UTEP, especially Lisette and Briandy, for the laughter and wonderful times we shared together. Your friendship has been a source of joy throughout my journey. I am also thankful to Dr. Jyoti and Dr. Gabriela for their support and friendship since my time at UTEP.

Above all, I am indebted to my family, whose love and support have been invaluable. Their belief in me has kept me going, and this journey would not have been possible without them. I am also grateful to all my friends for their encouragement and companionship.

A very special thank you goes to my husband, M.S. Dayan Viera, for always being by my side, supporting me in every step, and being my friend as well. This journey would not have been possible without your assistance.

Table of Contents

List of Figures

Introduction

1.1 Antibiotic Resistance

Antibiotics have been a tremendous boon to humanity, enabling us to combat infections and microbial threats. However, the issue of antibiotic resistance emerged shortly after the first antibiotic was discovered, posing a significant challenge. Today, antibiotic resistance stands as one of the gravest global threats we face. In the United States alone, every year, a minimum of 2.5 million infections and approximately 35,000 deaths can be attributed to bacteria strains that have developed resistance to antibiotics (Kadri, 2020).

Bacteria employ their genetic adaptability to withstand the inhibitory effects of antibiotics by acquiring genetic material, undergoing mutations, and modifying the expression of their genome. This acquired antibiotic resistance gene can be transferred from one bacterium to another through division processes or horizontal gene transfer. On average, bacterial resistance to a specific antibiotic develops and evolves within approximately 50 years after the antibiotic's initial use. Although antibiotic resistance is a natural process that occurs gradually through genetic changes, human activities have expedited this process through various anthropogenic factors. (Sharma et al., 2016). Both gram-negative and gram-positive pathogens have experienced an increase in antibiotic resistance. While the development of antibiotic resistance typically proceeds slowly through genetic changes, the overuse and misuse of antibiotics serve as significant drivers that accelerate this process. Bacteria have evolved various types of resistance mechanisms to overcome the inhibitory effects of antibiotics. Gaining a comprehensive understanding of the molecular aspects of these resistance mechanisms will provide valuable insights for the development of innovative therapeutic approaches to counteract resistance. (Wang et al., 2020)

1.2 Mechanisms of antibiotic resistance.

Antimicrobial resistance mechanisms can be categorized into four groups: active drug efflux pumps, target drug modification, drug inactivation, and regulation of drug uptake. The specific mechanisms employed vary between gram-positive and gram-negative bacteria. Gram-negative bacteria typically utilize all four mechanisms, while gram-positive bacteria have a limited ability to regulate drug uptake and may lack certain types of active drug efflux pumps. The dissemination of resistance genes and antibiotic resistance occurs through processes such as transformation, transduction, and conjugation. Figure 1 provides an overview of general resistance mechanisms. (Munita & Arias, 2016)

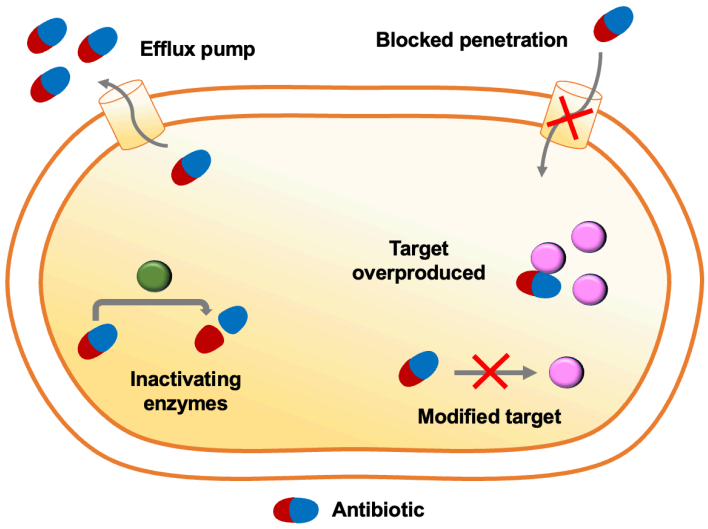

Figure 1. *Antibiotic Resistance Mechanisms in Bacteria.*

1.3 Strategy to combat antibiotic resistance, specifically environment to clinic.

Exploring the presence of resistance genes in disease-causing clinical pathogens plays a crucial role in combating antibiotic resistance. The Antibiotic Resistance Genes Database (ARDB) in 2009 contained approximately 13,293 genes known to confer resistance to various antibiotics. (Liu & Pop, 2009). It has been hypothesized that these resistance genes in clinical pathogens originate

from drug-producing organisms found in the environment. (Ogawara, 1981). For instance, aminoglycoside resistance enzymes encoded by *Streptomyces kanamyceticus* showed identical biochemical activity to those found in clinical isolates of *Escherichia coli* and *Pseudomonas aeruginosa* (Poole, 2005) (Davis et al., 2010). However, resistance genes can undergo multiple rounds of evolution during the gene transfer process between the environmental resistome and clinical settings. Another example is the transfer of the class-A extended-spectrum β-lactamase CTX-M gene from environmental *Kluyvera spp*. to clinical pathogens. Recent research using a metagenomic approach identified seven genes originating from non-pathogenic soil bacteria that were 100% identical to resistance genes in clinical pathogens, including resistance against β-lactams, tetracyclines, aminoglycosides, sulfonamides, and chloramphenicol (Forsberg et al., 2012). The amino acid composition of aminoglycoside phosphotransferase APH (3') enzyme showed 100% identity between clinical isolates of gram-negative and gram-positive pathogens and environmental *Bacillus circulans* and *Streptomyces fradiae* bacteria. (Lu et al., 2021) (Alekseeva et al., 2019). The shared niche between environmental microbes and pathogens serves as the most likely site for the transfer of resistant genes. Identifying and mapping antibiotic resistance genes in non-pathogenic environmental microbes is a critical step in slowing the emergence of antibiotic-resistant pathogens in clinical settings.

1.3.1 *Streptomyces* soil bacteria harbor a reservoir of antibiotic resistance genes.

The majority of clinically approved antibiotics, such as streptomycin, tetracycline, erythromycin, neomycin, and gentamycin, are derived from actinomycetes, a group of gram-positive filamentous bacteria commonly found in soil. (Van der Meij et al., 2017). Actinomycetes, particularly the genus *Streptomyces*, are responsible for producing approximately 70% of clinically useful antibiotics as secondary metabolites. *Streptomyces* bacteria are characterized by their filamentous morphology

and high guanine + cytosine (G+C) content in their genome, resembling fungi. (Tan et al., 2016) By studying the self-resistance mechanisms within antibiotic-producing bacteria, we can gain insights to impede the transfer of environmental genes to clinical pathogens. Among *Streptomyces* species, *S. griseus*, utilized for industrial streptomycin production, and *S. coelicolor*, employed in genetic studies, have been extensively investigated. (Jones & Elliot, 2017). Many of the resistance genes in *Streptomyces* are found within the same cluster as the antibiotic biosynthesis genes. These resistance genes are often located on the stable plasmid A and can be readily transferred to other strains through conjugation.

1.3.2 Echinomycin: synthesized by the bacterium *Streptomyces lasalocidi.*

Secondary metabolites produced by *Streptomyces* are nonribosomal peptides with a wide range of biological functions, including antimicrobial, antitumor, cytostatic, immunosuppressant, pigment, and antiviral activities (Du et al., 2000; Komaki et al., 2018). Unlike peptides synthesized by ribosomal machinery, these nonribosomal peptides are produced by a large enzyme complex called nonribosomal peptide synthetase (NRPS) through a thiol-templated mechanism. NRPSs have the ability to synthesize linear or cyclic peptides that may contain N-methylated and D-amino acids, as well as fatty acids attached at the N-terminus (Zhu et al., 2014). While NRPSs can be found in all three domains of life, they are most prevalent in bacteria, less common in eukaryotes, and rare in archaea (An et al., 2022). The gene cluster responsible for nonribosomal peptide biosynthesis typically includes regulatory genes and self-resistance genes, which play a role in protecting the host organism from the toxic compounds they produce (Lautru et al., 2005).

Echinomycin, derived from *Streptomyces echintus*, is a cyclic octadepsipeptide antibiotic with two quinoxaline rings that bisintercalate into double-stranded DNA. It specifically binds to CpG steps in the DNA, inhibiting replication and transcription. Structural studies reveal hydrogen bonding

between alanine residues in echinomycin and the guanine base in CpG, as well as unique base pairing in the AT regions. Echinomycin's binding affinity to DNA is influenced by flanking sequences around the CpG site (Kong et al., 2005; Van Dyke & Dervan, 1984). It has been investigated in clinical trials for cancer treatment and exhibits additional effects such as apoptosis induction, cell signaling inhibition, and hypoxia-inducible factor (HIF)-1α inhibition. Nanoliposomal-echinomycin has shown promise in inhibiting HIF-1α and eliminating triple-negative breast cancer (Bailey et al., 2020).

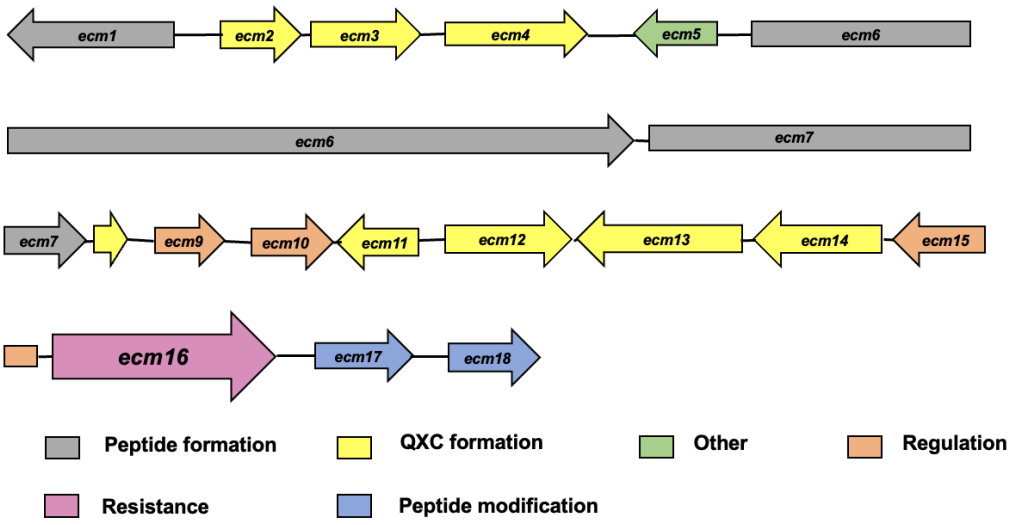

Figure 2. *Echinomycin Biosynthesis Gene Cluster Isolated from Streptomyces lasaliensis. (Gade, 2021)*

Echinomycin also demonstrates antimicrobial activity against human-associated pathogens, although its self-resistance mechanism is important to understand. The 36-kb echinomycin biosynthetic gene cluster from *S. lasalocidi* linear plasmid includes eight genes responsible for quinoxaline-2-carboxylic acid (ecm2, ecm3, ecm4, ecm8, ecm11, ecm12, ecm13, and ecm14), as well as five genes involved in backbone formation and modification (ecm1, ecm6, ecm7, ecm17,

and ecm18) (Watanabe et al., 2006). The echinomycin biosynthetic gene cluster also contains a self-resistance gene, ecm16, which was identified (Figure 2) . Overexpression of ecm16 in the engineered echinomycin-producing strain resulted in a significant increase in antibiotic production (Gade et al., 2023). The function of Ecm16 in the biosynthesis gene cluster of echinomycin antibiotic isolated from *S. lasalocidi* remains unclear.

1.4 Ecm16 crystal structure.

In a recent study by Gade et al. (Gade et al., 2023), they propose a potential mechanism by which Ecm16 functions independently in DNA repair, separate from the NER (Nucleotide Excision Repair) system. The researchers demonstrated that expressing Ecm16 alone is enough to provide resistance against echinomycin, even in *E. coli* K12, which is otherwise sensitive to echinomycin. Their findings revealed that the DNA-binding capability and ATP hydrolysis activity of Ecm16 are essential for its ability to confer resistance. These characteristics align with the crystal structure of Ecm16 (Figure 3) (Gade et al., 2023), which exhibits four nucleotide binding sites and a prominent DNA-binding groove on its ventral side.

1.5 Crystal Structure of Ecm16 is Similar to UvrA of Nucleotide Excision Repair

Ecm16, an uncharacterized protein, is believed to play a role in self-protection against echinomycin. This hypothesis is supported by its sequence similarity of approximately 30% to prokaryotic UvrA proteins (Gade et al., 2023) (Figure 4), which are known to function in the NER (Nucleotide Excision Repair) pathway. (Watanabe et al., 2006). The NER pathway plays a crucial role in repairing bulky DNA damage, such as UV lesions or benzo[a]pyrene adducts, although it exhibits a wide range of DNA repair activities. The conservation of this pathway extends across both prokaryotic and eukaryotic organisms.

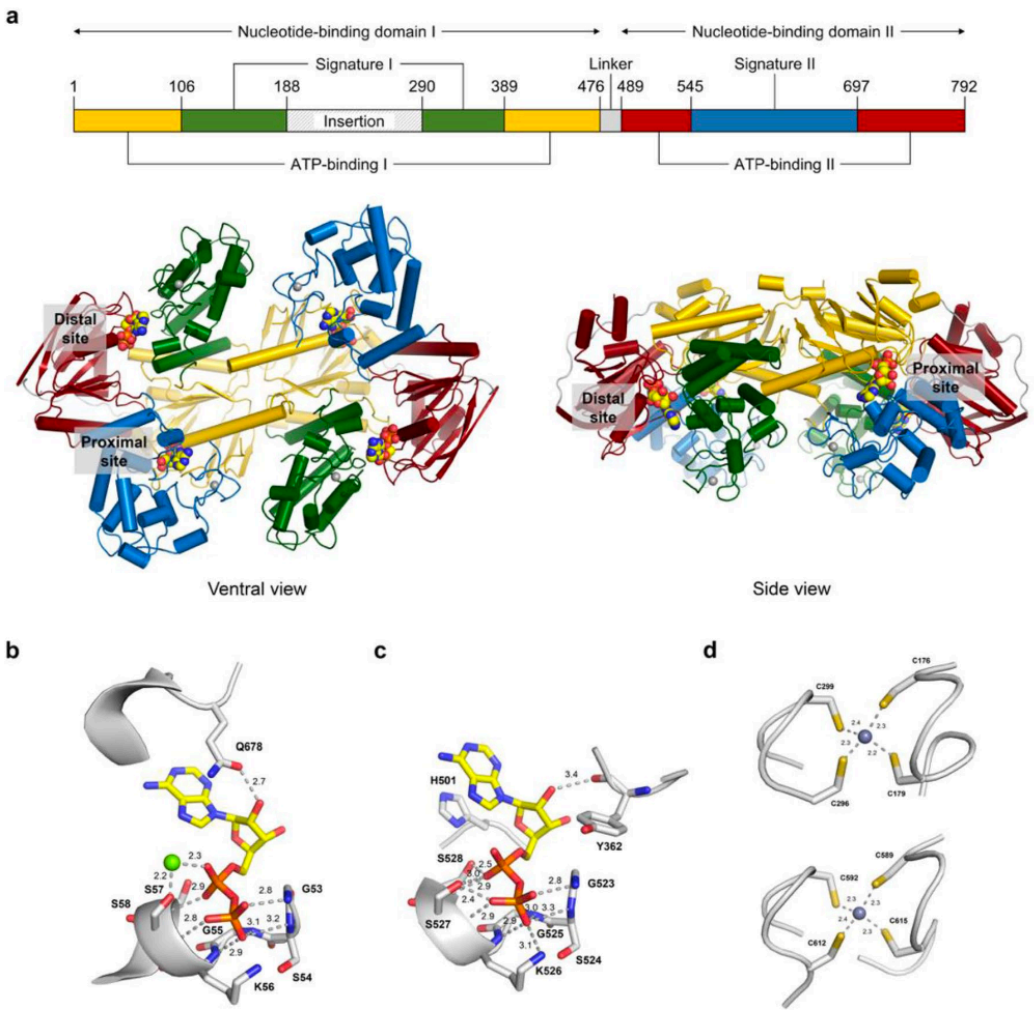

Figure 3. *Crystal structure of Ecm16. (a) Domain organization and overall architecture of the Ecm16 homodimer. While the primary structure contains an insertion domain, it is not observed in the crystal structure. Spheres are used to represent ADP, Zn^{2+}, and Mg^{2+} atoms (C: yellow, N: blue, O: red, P: orange, Zn: grey, Mg: green). (b) The proximal nucleotide-binding site is depicted, and atom-to-atom distances are provided in angstroms (Å). (c) The distal nucleotide-binding site is displayed. (d) The top section showcases zinc-binding module 2, while the bottom section showcases zinc-binding module 3. (Adapted from Gade et al., 2023).*

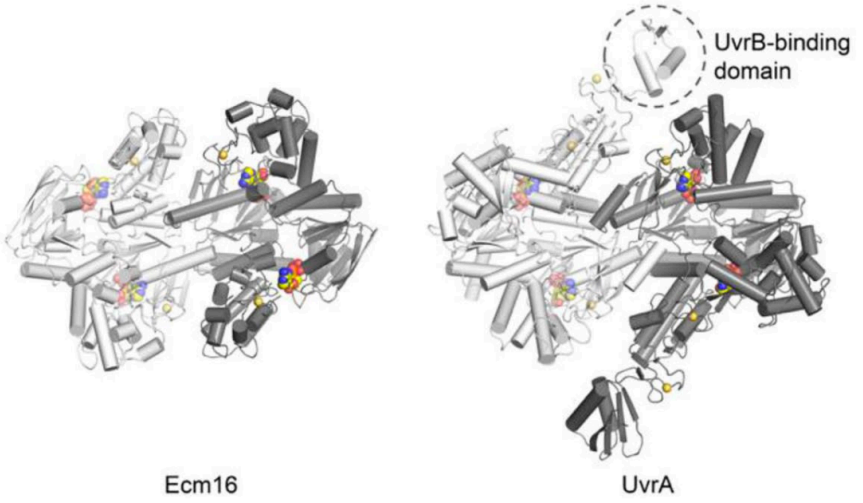

Figure 4. *Crystal structure of Ecm16 (PDB ID: 3SH1) from Streptomyces lasalocidi and UvrA (PDB ID: 2R6F) from Bacillus stearothermophilus is depicted in the following manner: Each monomer is distinguished by dark and light grey colors. The nucleotides are illustrated using a ball and stick model, while the zinc ions are represented as orange spheres (Adapted from Gade et al., 2023).*

The recognition and cleavage of DNA damage by UvrA, UvrB, UvrC and UvrD proteins involve a multistep process that is ATP-dependent (de Laat et al., 1999). UvrA forms a homodimer in an ATP-dependent manner and interacts with UvrB to form either a UvrA2B or UvrA2UvrB2 complex. UvrA is responsible for scanning DNA and recognizing damage. It recruits UvrB, which separates the two strands of DNA, and then recruits UvrC, an endonuclease, to the site of the lesion. UvrC cleaves the phosphodiester bond eight nucleotides upstream and up to five nucleotides downstream of the modified nucleotide. UvrC then recruits UvrD, which displaces the cleaved DNA fragment. Finally, DNA polymerase I synthesizes the missing DNA sequence using the undamaged complementary strand, and DNA ligase seals the breaks, completing the repair process (Figure 5) (Truglio et al., 2006). The NER pathway can repair various DNA lesions,

including pyrimidine dimers, unpaired T and G residues, backbone modifications such as single nucleotide gaps and nicks, as well as adducts of anthramycin, cholesterol, fluorescein, and polypeptides (Sabarinathan et al., 2016). The broad substrate specificity of NER can be attributed to UvrA, the damage sensor component of NER. Ecm16, similar to UvrA2 (Erlandson, Gade, Kim, et al., 2022), lacks the UvrB-binding domain and the associated Zn-binding module 1, which are typically present in all class I UvrA proteins. However, the three-dimensional structure of Ecm16, UvrA, and UvrA2 shows high homology, suggesting that these proteins employ a similar mechanism for DNA-substrate recognition and binding.

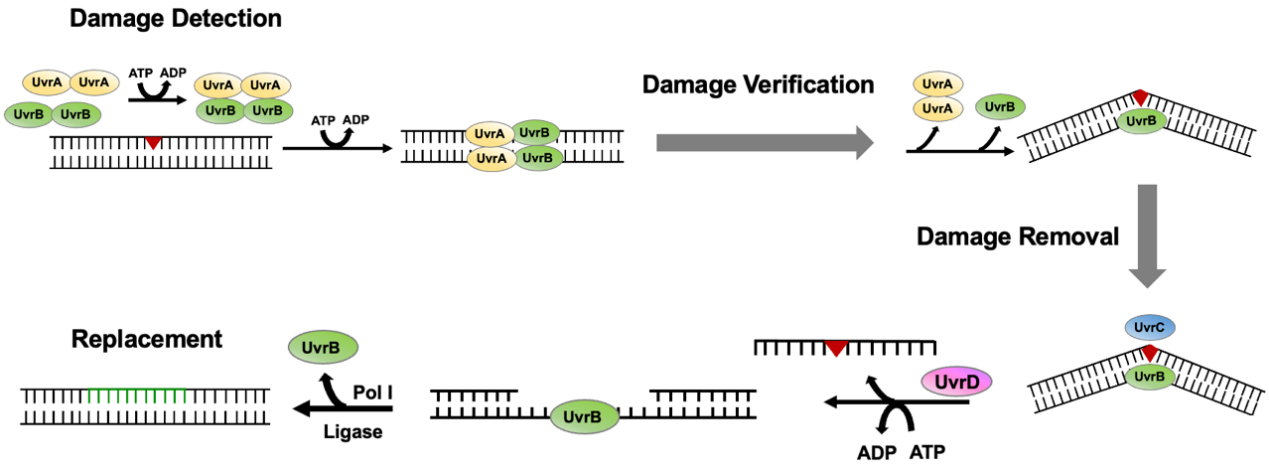

Figure 5. *Schematic overview of the prokaryotic nucleotide excision repair pathway, depicting the progression from damage recognition to damage verification, and finally to damage removal and resynthesis.*

Despite its structural resemblance to UvrA, Ecm16 was unable to complement the DNA repair activity of UvrA specifically against UV radiation-induced DNA damage. Additionally, Ecm16 was able to confer echinomycin resistance to host cells lacking UvrB, UvrC, or UvrD, which indicates that Ecm16 operates independently of the NER machinery for its function (Erlandson,

Gade, Menikpurage, et al., 2022). This suggests that Ecm16 has a distinct mode of action in DNA repair, offering a potential alternative pathway or mechanism for countering the effects of DNA damage caused by echinomycin (Gade et al., 2023).

1.6 Role of ATP binding and hydrolysis activity of Ecm16

Gade et al. (Gade, 2021) examined the interactions of Ecm16 with both undamaged DNA and DNA substrates bound to echinomycin, focusing on the roles of the proximal and distal nucleotide binding sites in Ecm16 in its antibitic reistance mechanism. To examine the impact of crucial amino acid residues within these binding sites of Ecm16, variant cultures were created with substitutions in the proximal and distal ATP binding sites (K56A, K526A) as well as the ATP hydrolysis sites (E399Q, E708Q and E399Q, E708Q). The variant cultures were cultivated in a nutrient-rich liquid medium (LB) supplemented with Ampicillin and 0.2% Arabinose. Incubation took place at a temperature of 37°C and a speed of 200 rpm. Optical density readings were recorded every 30 minutes over a period of 6 hours using a Thermo UV-Vis Spectrophotometer (Gade, 2021). The results demonstrated that in vivo, none of the Ecm16 variants with compromised ATP binding or hydrolysis displayed the capability to confer echinomycin resistance to *E. coli* cells. The lysine residue, located in the Walker A motif, is known for its interaction with the β and γ phosphate groups in different NTPases. Similarly, the conserved glutamate residue within the Walker B motif can polarize an incoming water molecule, which plays a role in attacking the γ-phosphate during ATP hydrolysis. Based on these observations, the researchers proposed the hypothesis that replacing this glutamate residue with glutamine in Ecm16 would greatly inhibit ATP hydrolysis, effectively trapping the protein in an active ATP-bound conformation (Gade, 2021), which holds critical significance in elucidating the mechanism of antibiotic resistance mediated by Ecm16.

Building upon this concept, my research revolves around investigating the Ecm16E399Q,E708Q Ecm16 double mutant, specifically designed to impact nucleotide hydrolysis. Our hypothesis posits that Ecm16 accomplishes its function by undergoing conformational changes driven by the processes of ATP binding and hydrolysis.

Specific Aims:

1. How does Ecm16 scan the DNA?
2. How does Ecm16 do the repair?

Materials and Methods

2.1 Plasmid Construction and Ecm16E399Q,E708Q Expression.

Ecm16E399Q,E708Q was cloned between the restriction enzyme digestion sites NdeI and EcoRI using the PCR based method of Restriction-Free (RF) cloning followed by DpnI enzyme digestion, transformation, and screening of positive clones. The Ecm16E399Q,E708Q gene was subcloned into a pET-28a(+) expression vector between the restriction enzyme sites NdeI and EcoRI at the 5' and 3' end, respectively. The Ecm16E399Q,E708Q-pET28a (+) construct was introduced into *E. coli* strain BL21-DE3 and plated on an LB agar plate supplemented with 50 μg/ml kanamycin antibiotic. Subsequently, 2-3 colonies were selected from the plate and inoculated into 5 or 10 ml of LB broth containing 50 μg/ml kanamycin, and the culture was allowed to grow overnight at 37°C and 200 rpm. Once the optical density at 600 nm (OD600) reached the desired expression level (0.6-0.8), the cells were induced by adding 0.2 mM isopropyl β-D-1- thiogalactopyranoside (IPTG), and the temperature was lowered to 18°C in the shaker-incubator. The recombinant Ecm16 protein was expressed by transforming *E. coli* BL21 (DE3) host strains with the recombinant pET28a constructs encoding the wild-type Ecm16. The cells were grown in 5 ml of LB medium supplemented with kanamycin at a temperature of 37°C until they reached an optical density of approximately 0.6-0.8 at 600 nm. Protein expression was induced by adding 0.1 mM IPTG, and the culture was further incubated for 16 hours at 18°C and 200 rpm.

2.2 Ecm16E399Q,E708Q protein purification

Cell pellet was resuspended in lysis buffer containing 50 mM HEPES (pH 7.5), 200 mM NaCl, 10% glycerol, 10 mM Phenylmethylsulphonyl fluoride (PMSF), 10 μg/ml DNase, and 10 mM

$MgCl_2$. Cell disruption was achieved using sonication with a Branson Ultrasonics instrument, followed by removal of cell debris through centrifugation at 15,000 g for 45 minutes at 4°C. The resulting cleared cell lysate was then applied to a 5 ml His-Trap Crude column (GE Healthcare) that had been pre-equilibrated with a loading buffer consisting of 50 mM HEPES at pH 7.5 and 200 mM NaCl. The protein was eluted with a step gradient of imidazole (250 mM) using elution buffer (50 mM HEPES pH 7.5, 200 mM NaCl, 500 mM Imidazole). Ecm16 E399Q,E708Q eluted from the nickel column was diluted up to 10- fold using dilution buffer (50 mM HEPES pH 7.5, 50 mM NaCl). The diluted protein was applied to 5 ml Hi-Trap QHP anion-exchange column (GE Healthcare). Protein was eluted with 5 column volumes (CV) linear NaCl gradient from 50 mM to 500 mM concentration. The protein was concentrated up to 6 mg/ml and gel filtration was performed on Superdex 200 10/300 GL (GE Healthcare) equilibrated with storage buffer (50 mM HEPES pH 7.5, 50 mM NaCl). After elution, the protein sample was concentrated to a final concentration of 10 mg/ml. Subsequently, it was rapidly frozen in liquid nitrogen to preserve its integrity and stored at -80°C for future use.

2.3 Crystallization trial of Ecm16E399Q,E708Q

A total of approximately 900 conditions from commercially available screens (Molecular dimensions, Hampton Research) were screened using an NT8 (Formulatrix) crystallization robotic system. The protein drop size of 200 µL (2 and 4 mg/ml) and 200 uL of the crystallization condition were dispensed into 96-well sitting drop plates (ARI, Intelli). The initial hit was observed after 10 days, and subsequent efforts were made to reproduce and optimize the protein concentration, buffer pH, percentage of precipitant, and additives to obtain well-diffracting crystals. The optimal crystals of Ecm16E399Q,E708Q were cultivated at 18°C using vapor diffusion in hanging drops, by

combining 2 µl of Ecm16E399Q, E708Q (10 mg/ml) with 2 µl of equilibration buffer (0.1 M MES pH 6.5, 0.1M Imidazole, 0.03M Magnesium chloride hexahydrate, 0.03 M calcium chloride dihydrate, and 43% (w/v) GOL-P4K). To ensure cryoprotection, the crystals were transferred into the same buffer containing 20% v/v ethylene glycol before being flash-frozen.

2.4 X-Ray preliminary data collection of Ecm16E399Q,E708Q

The diffraction data set was obtained at the BL12-2 microfocus beamline at Stanford Synchrotron Radiation Lightsource, with data collection carried out at a temperature of 100K. Data reduction was conducted using the XDS program suite (Potterton et al., 2018). To perform molecular replacement, a search model based on the Ecm16 structure (PDB: 7SH1). The PHASER program from the CCP4 suite was employed for this purpose. The initial model was then built by tracing against the resulting electron density map obtained through molecular replacement. Crystallographic refinement was carried out using the iMosflm programs (Powell et al., 2017). Model building iterations were performed using COOT (Emsley & Cowtan, 2004). The final model comprises chain A (residues 15-80, 89-147, 173-180, 293-597, 605-791), chain B (residues 15-77, 88-150, 174-183, 297-598, 608-792), 4 ADP molecules, 2 Mg^{2+} ions, 4 Zn^{2+} ions.

2.5 Protein concentration determination

The protein concentrations in this study were determined using an Eppendorf Bio-spectrophotometer Basic, which involved measuring the absorbance at 280nm. The theoretical extinction coefficient calculated using ProtParam (Ecm16E399Q,E708Q - 40505 $M^{-1}cm^{-1}$) was considered during the concentration calculations.

Results

3.1 Expression of recombinant Ecm16E399Q,E708Q.

Ecm16E399Q,E708Q is a variant of the nucleotide hydrolase Ecm16. It was obtained through cloning between the restriction enzyme digestion sites NdeI and EcoRI, using the PCR-based method of Restriction-Free (RF) cloning (Bond & Naus, 2012). This was followed by DpnI enzyme digestion, transformation, and screening of positive clones. Confirmation of successful over-expression of the Ecm16E399Q,E708Q gene was obtained through the detection of a prominent band of approximately 86 kDa molecular size on SDS-PAGE, stained intensely with Coomassie dye. This band served as conclusive evidence for the presence of the desired protein product in the IPTG-induced sample. (Figure 6).

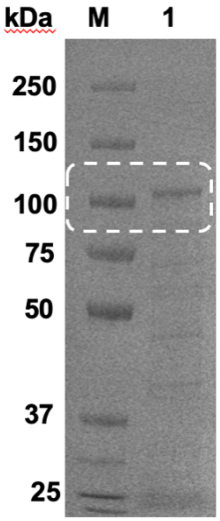

Figure 6. *SDS-PAGE analysis of expression of Ecm16E399Q,E708Q. Lines: M- Molecular weight marker, 1- Ecm16E399Q,E708Q expression.*

3.2 Purification of recombinant Ecm16E399Q,E708Q

To facilitate purification, the protein was expressed with N-terminal hexa-Histidine tags. This allowed for purification using immobilized metal affinity chromatography (IMAC). In the nickel-affinity chromatography step of purification, the N-terminal His-tag of the Ecm16E399Q,E708Q protein was bound to the nitrilotriacetic acid (NTA)-agarose resin of the column. This was confirmed by analyzing the flow-through sample in the SDS-PAGE gel (Figure 10). The Ecm16E399Q,E708Q was eluted using step gradient at 250 mM imidazole concentration (Figure 7).

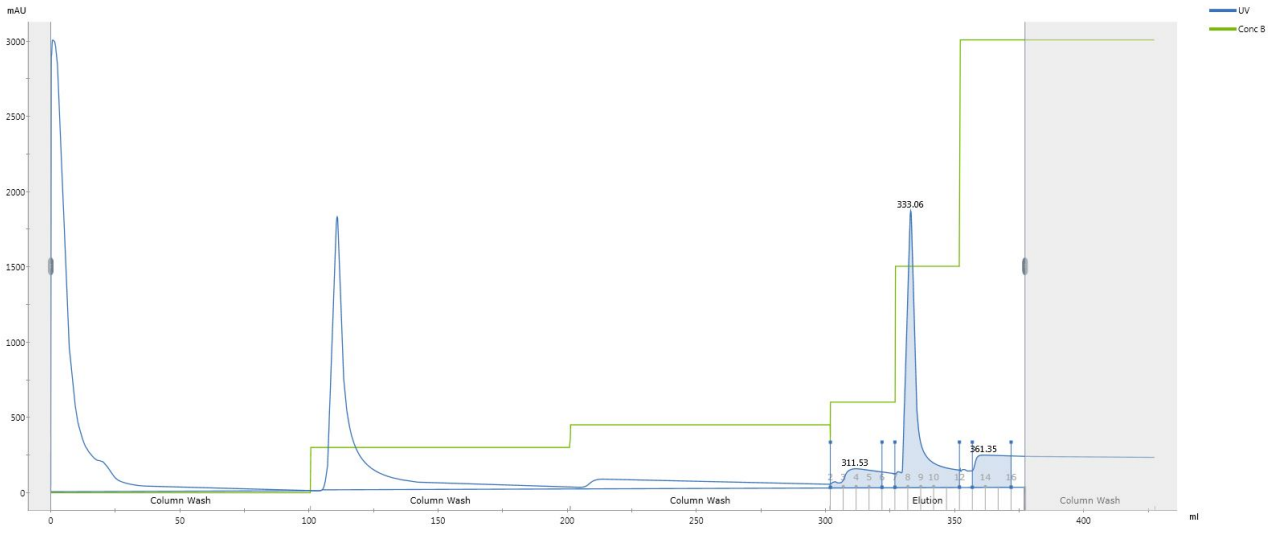

Figure 7. *Immobilized metal ion affinity chromatography of Ecm16E399Q,E708Q.*

Ion-exchange chromatography is a powerful technique for separating proteins based on their net surface charge. Anion exchange chromatography utilizes a positively charged stationary phase to facilitate the binding of proteins that carry a negative net surface charge. This separation technique takes advantage of the different surface charges exhibited by proteins with varying isoelectric point (pI) values at a specific pH. By applying a salt gradient, proteins can be separated based on their

affinity for the charged stationary phase. Proteins with a stronger affinity to the ion exchange matrix will elute under higher ionic strength conditions. We observed that addition of the DNase enzyme to the cell lysate shifts the NaCl concentration at which Ecm16E399Q,E708Q is eluted (Figure 8).

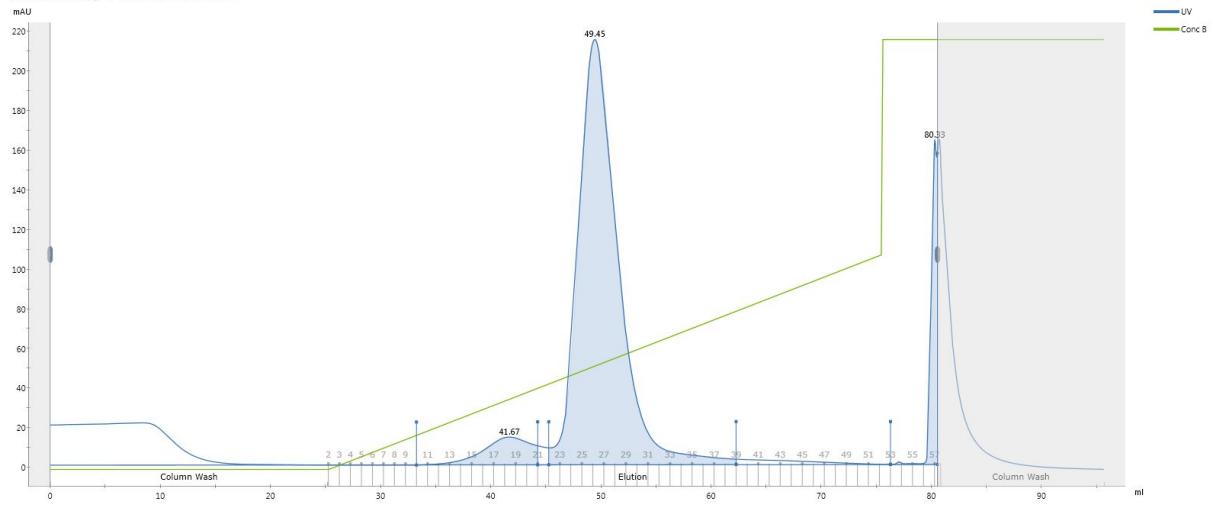

Figure 8. *Ion-exchange chromatography of Ecm16E399Q,E708Q.*

After purification using anion exchange chromatography (AEC), the protein was subsequently subjected to size exclusion chromatography (SEC). The purpose of SEC was to separate protein aggregates and obtain a homogeneous protein sample suitable for crystallographic studies (Figure 9). The successful preparation of His-tagged Ecm16E399Q,E708Q protein with a purity level greater than 90% was accomplished through a combination of affinity chromatography, anion exchange chromatography, and size exclusion chromatography. The confirmation of this result was obtained through analysis using SDS-Gel, as shown in Figure 10. Approximately, 2 mg of Ecm16E399QE708Q could be obtained from 1 liter of LB culture. Purified protein was flash frozen in liquid N_2 and stored at -80°C until needed.

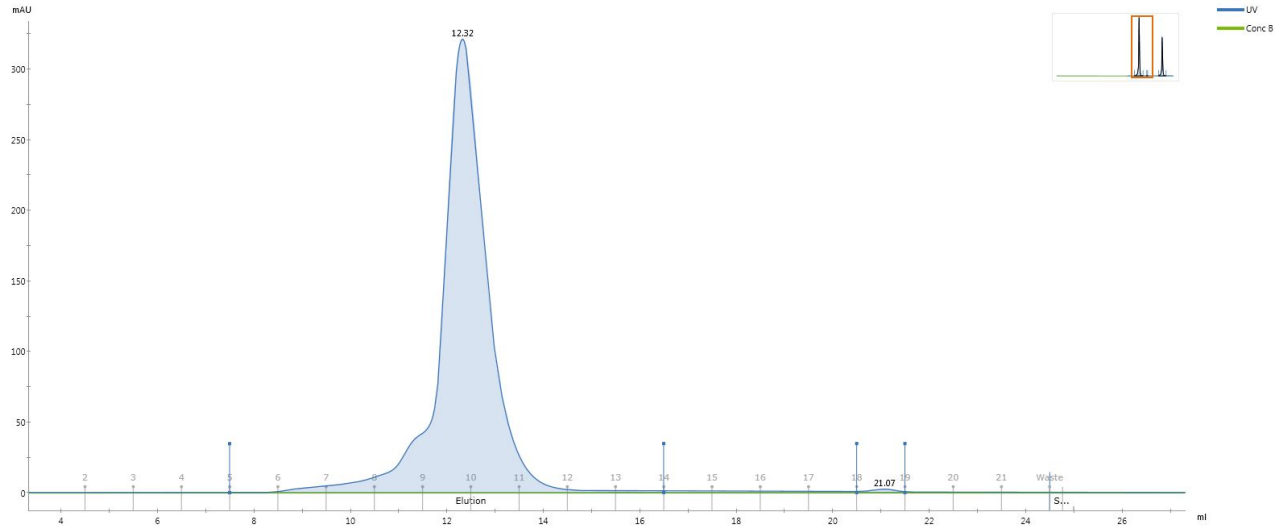

Figure 9. *Size Exclusion chromatography of Ecm16E399Q,E708Q.*

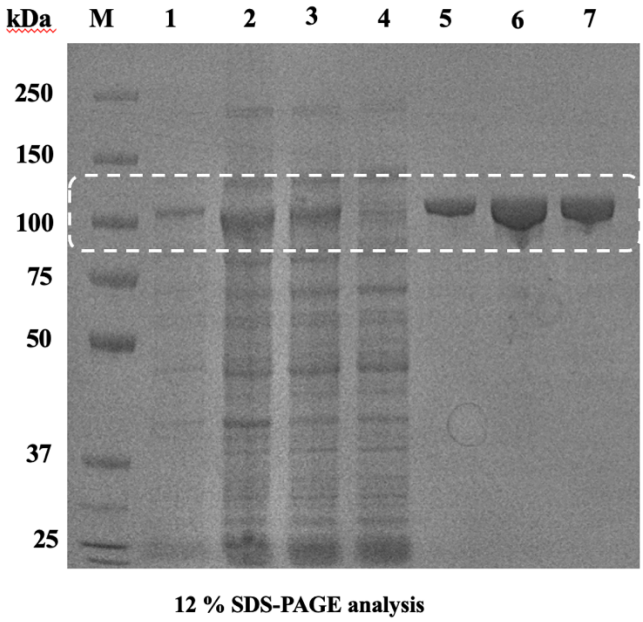

Figure 10. *SDS PAGE analysis of purified Ecm16E399Q,E708Q. Lanes: M- Molecular weight marker, 1- Ecm16E399Q,E708Q expression, 2- Ecm16E399Q,E708Q total cell lysate, 3- Soluble fraction of total cell lysate, 4- Flow-through IMAC, 5- IMAC purified protein, 6- AEC purified protein, 7- SEC purified protein.*

3.2 Crystallization experiments of Ecm16E399Q,E708Q

The initial crystal hit for Ecm16E399Q,E708Q was obtained, and further optimization efforts were employed to enhance crystal size (Figure 11 (a)). The optimization experiments encompassed the screening of various buffers and pH values ranging from 4 to 9, as well as different percentages of glycerol and PEG 4,000. An additive screen from Hampton Research was also utilized to improve crystal quality. Following the optimization process, well-formed rhombus-shaped crystals of Ecm16E399Q,E708Q appeared within three days and reached their full size in one week (Figure 11 (b)). These crystals were grown using the hanging-drop vapor diffusion method at 18°C, with a protein solution (10 mg/ml Ecm16E399Q,E708Q) mixed with an equal volume of a reservoir solution containing 0.1M MES/Imidazole at pH 6.5, 0.03M magnesium chloride hexahydrate/calcium chloride dihydrate, and 43% (w/v) GOL-PEG 4,000. To ensure cryoprotection, the crystals were soaked in a solution containing 20% (v/v) ethylene glycol before being flash-frozen in liquid nitrogen for X-ray diffraction analysis.

3.3 X-Ray diffraction studies of Ecm16E399Q,E708Q

Ecm16E399Q,E708Q crystallized in trigonal space group $P3_121$ with cell parameters a= 140.78 Å, b=140.78 Å, c=171.77 Å, α =90.0°, β =90.0°, γ=120.0°, and contained two molecules in the asymmetric unit (Table 3.1). Molecular replacement was performed using the iMosflm program (Powell et al., 2017) and the initial model was built using the resulting electron density map after molecular replacement followed by crystallographic refinement using program CCP4Interface 8.0.008 (Adams et al. 2010). Model-building was done by using program COOT (Emsley & Cowtan, 2004) with iterative sessions of refinement.

(a) (b)

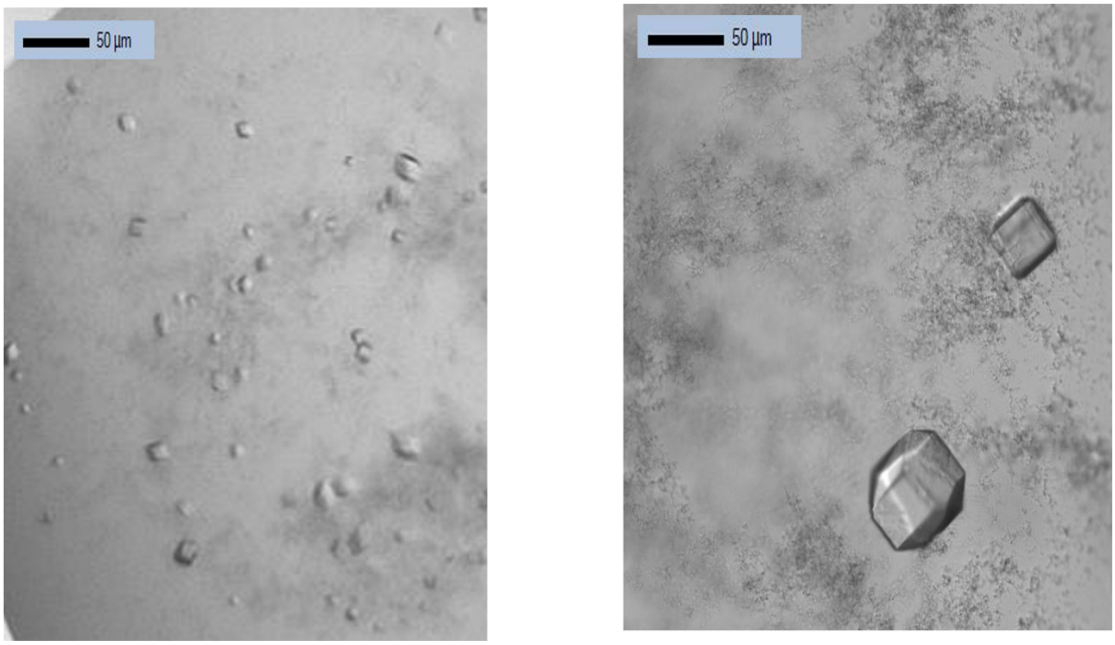

Figure 11. *(a). Initial Ecm16E399Q,E708Q crystals hit. (b) Optimized Ecm16E399Q,E708Q crystals.*

Using the molecular replacement method, the structure of Ecm16E399Q,E708Q was successfully determined at a resolution of 2.07 Å (Figure 12). The final model includes the Ecm16E399Q,E708Q homodimer, four adenosine diphosphate (ADP) molecules, two Mg^{2+} ions, and four Zn^{2+} ions. Due to ambiguous electron density, certain regions of Ecm16 were not included in the model, specifically residues 1-14, 81-88, 148-172, 181-292 (chain A), and residues 1-14, 78-87, 151-173, 184-296 (chain B). Notably, the missing sections correspond to the entire insertion domain, which aligns with the known flexibility of the insertion domain in class I UvrA proteins (Gade, 2021). The electron density analysis reveals the presence of ADP, rather than ATP, at both the proximal and distal nucleotide-binding sites.

Table 1. *Data Collection statistics*

Data Collection	**Ecm16E399Q,E708Q**
Beamline	BL12-2
Processing software	XDS
Wavelength (Å)	0.979
Resolution range (Å)	99.42-2.07
Space group	$P3_121$
Unit Cell a, b, c (Å)	140.78 140.78 171.77
Unit Cell α, β, γ (°)	90 90 120
Mean *I/sigma(I)*	3.1(0.1)
$CC_{1/2}$	0.612(0.117)
Completeness	95.3(92.8)

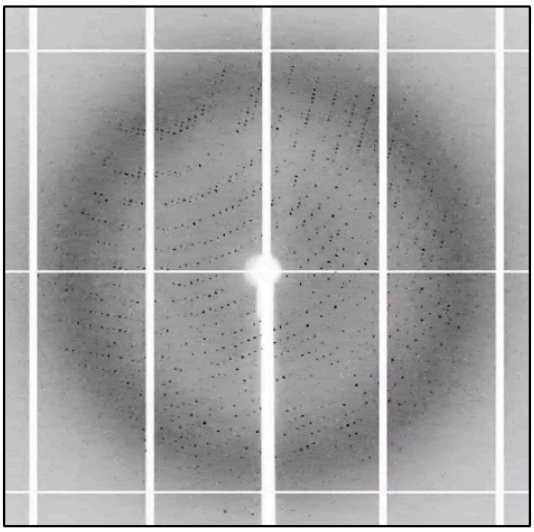

Figure 12. *Diffraction image for Ecm16E399Q,E708Q crystal.*

3.4 Nucleotide binding domain in Ecm16E399Q,E708Q

The Ecm16E399Q,E708Q protein forms a homodimer arrangement where the two protomers are positioned in a head-to-head orientation. Each protomer consists of two ABC ATPase motifs, namely nucleotide-binding domain I and II (NBD-I and NBD-II). To investigate whether the crystal structure represents the active ATP-bound conformation of the protein, we performed a substitution experiment. We replaced the ADP molecules in the density corresponding to the nucleotide binding domains of each monomer with ATP (Figure 13). However, the observed density surrounding the β and γ phosphate regions of ATP appeared red, indicating that it did not correspond to ATP molecules (Stewart et al., 2008). Conversely, when we replaced the ATP

molecules with ADP in the same nucleotide binding domain sites (Figure 13), we observed blue density, confirming that the ADP molecules were consistent with the observed NBD density.

(a)

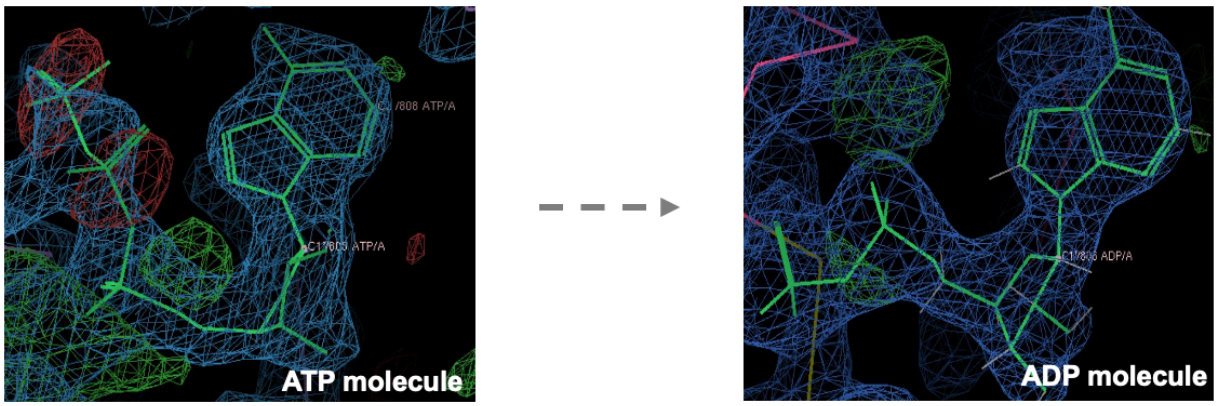

(b)

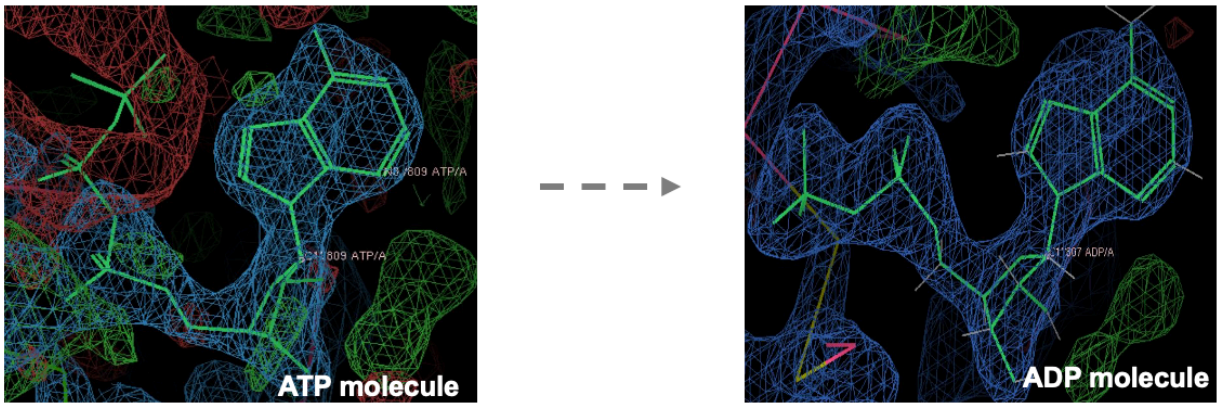

Figure 13. *Nucleotide binding domains per monomer: (a) NBD-I and (b) NBD-II with ATP and ADP bound to Ecm16E399Q,E708Q.*

Conclusion and Future exeriments

We achieved successful expression and purification of 6x Histidine Tagged-Ecm16E399Q, E708Q from *E. coli*. Subsequently, we employed X-ray crystallography to determine the structure of Ecm16E399Q, E708Q with a high resolution of 2.07 Å. The crystallographic analysis uncovered that both nucleotide binding domains (NBDs) of Ecm16E399Q,E708Q were found to contain ADP-bound. This structural revelation indicates that the strategic mutations performed in this research were insufficient to obtain the desired ATP-bound state in the NBDs. The obtained structural information highlights the need for further modifications or investigations to achieve the desired ATP-bound conformation in Ecm16E399Q,E708Q NBDs.

Ecm16 regulates its ATPase activity based on the type of DNA substrate (damaged vs. undamaged), and its insertion domain plays a crucial role in this regulatory process. Therefore, it is crucial to obtain the ATP-bound state in our mutant structure. To achieve this, we have proposed a series of experiments that we will perform as follows:

1. Incubation at room temperature for 20 minutes: We will incubate Ecm16E399Q,E708Q with 1mM $MgCl_2$ / 1mM ATP, Ecm16E399Q,E708Q with 1mM $MgCl_2$ / 3mM ATP, and Ecm16E399Q,E708Q with 3mM $MgCl_2$ / 3mM ATP (Sherman et al., 2014) .

2. Co-Crystallization at 4°C: We will perform co-crystallization experiments by combining Ecm16E399Q,E708Q with 1mM $MgCl_2$ / 1mM ATP, Ecm16E399Q,E708Q with 1mM $MgCl_2$ / 3mM ATP, and Ecm16E399Q,E708Q with 3mM $MgCl_2$ / 3mM ATP (Stefan et al., 2020).

3. Incubation at 4°C for 1 hour: We will incubate Ecm16E399Q,E708Q with 1mM ATP and Ecm16E399Q,E708Q with 3mM ATP for one hour at 4°C (Borsellini et al., 2022).

4. Soaking: We will perform soaking experiments by exposing Ecm16E399Q,E708Q to 1mM ATP and Ecm16E399Q,E708Q to 3mM ATP (Goepfert et al., 2013).

5. Addition of 1mM EDTA to all buffer purifications (Simpson et al., 2019).

References

Alekseeva, M. G., Boyko, K. M., Nikolaeva, A. Y., Mavletova, D. A., Rudakova, N. N., Zakharevich, N. V., Korzhenevskiy, D. A., Ziganshin, R. H., Popov, V. O., & Danilenko, V. N. (2019). Identification, functional and structural characterization of novel aminoglycoside phosphotransferase APH (3 ″)-Id from Streptomyces rimosus subsp. rimosus ATCC 10970. *Archives of biochemistry and biophysics*, *671*, 111-122.

An, J. S., Kim, M.-S., Han, J., Jang, S. C., Im, J. H., Cui, J., Lee, Y., Nam, S.-J., Shin, J., & Lee, S. K. (2022). Nyuzenamide C, an Antiangiogenic Epoxy Cinnamic Acid-Containing Bicyclic Peptide from a Riverine Streptomyces sp. *Journal of Natural Products*, *85*(4), 804-814.

Bailey, C. M., Liu, Y., Peng, G., Zhang, H., He, M., Sun, D., Zheng, P., Liu, Y., & Wang, Y. (2020). Liposomal formulation of HIF-1α inhibitor echinomycin eliminates established metastases of triple-negative breast cancer. *Nanomedicine: Nanotechnology, Biology and Medicine*, *29*, 102278.

Bond, S. R., & Naus, C. C. (2012). RF-Cloning. org: an online tool for the design of restriction-free cloning projects. *Nucleic acids research*, *40*(W1), W209-W213.

Borsellini, A., Kunetsky, V., Friedhoff, P., & Lamers, M. H. (2022). Cryogenic electron microscopy structures reveal how ATP and DNA binding in MutS coordinates sequential steps of DNA mismatch repair. *Nature structural & molecular biology*, *29*(1), 59-66.

Davis, M. A., Baker, K. N., Orfe, L. H., Shah, D. H., Besser, T. E., & Call, D. R. (2010). Discovery of a gene conferring multiple-aminoglycoside resistance in Escherichia coli. *Antimicrobial agents and Chemotherapy*, *54*(6), 2666-2669.

de Laat, W. L., Jaspers, N. G., & Hoeijmakers, J. H. (1999). Molecular mechanism of nucleotide excision repair. *Genes & development*, *13*(7), 768-785.

Du, L., Sánchez, C., Chen, M., Edwards, D. J., & Shen, B. (2000). The biosynthetic gene cluster for the antitumor drug bleomycin from Streptomyces verticillus ATCC15003 supporting functional interactions between nonribosomal peptide synthetases and a polyketide synthase. *Chemistry & biology*, *7*(8), 623-642.

Emsley, P., & Cowtan, K. (2004). Coot: model-building tools for molecular graphics. *Acta Crystallographica Section D: Biological Crystallography*, *60*(12), 2126-2132.

Erlandson, A., Gade, P., Kim, C.-Y., & Mera, P. (2022). Class II UvrA protein Ecm16 requires ATPase activity to render resistance against echinomycin. *bioRxiv*, 2022.2002. 2002.478902.

Erlandson, A., Gade, P., Menikpurage, I. P., Kim, C. Y., & Mera, P. E. (2022). The UvrA-like protein Ecm16 requires ATPase activity to render resistance against echinomycin. *Molecular Microbiology*, *117*(6), 1434-1446.

Forsberg, K. J., Reyes, A., Wang, B., Selleck, E. M., Sommer, M. O., & Dantas, G. (2012). The shared antibiotic resistome of soil bacteria and human pathogens. *science*, *337*(6098), 1107-1111.

Gade, P., Erlandson, A., Ullah, A., Chen, X., Mathews, I. I., Mera, P. E., & Kim, C.-Y. (2023). Structural and functional analyses of the echinomycin resistance conferring protein Ecm16 from Streptomyces lasalocidi. *Scientific reports*, *13*(1), 7980.

Gade, P. R. (2021). Molecular Mechanism Of Dna Bisintercalator Antibiotic Resistance.

Goepfert, A., Stanger, F. V., Dehio, C., & Schirmer, T. (2013). Conserved inhibitory mechanism and competent ATP binding mode for adenylyltransferases with Fic fold. *PloS one*, *8*(5), e64901.

Jones, S. E., & Elliot, M. A. (2017). Streptomyces exploration: competition, volatile communication and new bacterial behaviours. *Trends in microbiology*, *25*(7), 522-531.

Kadri, S. S. (2020). Key takeaways from the US CDC's 2019 antibiotic resistance threats report for frontline providers. *Critical care medicine*.

Komaki, H., Sakurai, K., Hosoyama, A., Kimura, A., Igarashi, Y., & Tamura, T. (2018). Diversity of nonribosomal peptide synthetase and polyketide synthase gene clusters among taxonomically close Streptomyces strains. *Scientific reports*, *8*(1), 6888.

Kong, D., Park, E. J., Stephen, A. G., Calvani, M., Cardellina, J. H., Monks, A., Fisher, R. J., Shoemaker, R. H., & Melillo, G. (2005). Echinomycin, a small-molecule inhibitor of hypoxia-inducible factor-1 DNA-binding activity. *Cancer research*, *65*(19), 9047-9055.

Lautru, S., Deeth, R. J., Bailey, L. M., & Challis, G. L. (2005). Discovery of a new peptide natural product by Streptomyces coelicolor genome mining. *Nature chemical biology*, *1*(5), 265-269.

Liu, B., & Pop, M. (2009). ARDB—antibiotic resistance genes database. *Nucleic acids research*, *37*(suppl_1), D443-D447.

Lu, W., Li, K., Huang, J., Sun, Z., Li, A., Liu, H., Zhou, D., Lin, H., Zhang, X., & Li, Q. (2021). Identification and characteristics of a novel aminoglycoside phosphotransferase, APH (3′)-IId, from an MDR clinical isolate of Brucella intermedia. *Journal of Antimicrobial Chemotherapy*, *76*(11), 2787-2794.

Munita, J. M., & Arias, C. A. (2016). Mechanisms of antibiotic resistance. *Virulence mechanisms of bacterial pathogens*, 481-511.

Ogawara, H. (1981). Antibiotic resistance in pathogenic and producing bacteria, with special reference to beta-lactam antibiotics. *Microbiological reviews*, *45*(4), 591-619.

Poole, K. (2005). Aminoglycoside resistance in Pseudomonas aeruginosa. *Antimicrobial agents and Chemotherapy*, *49*(2), 479-487.

Potterton, L., Agirre, J., Ballard, C., Cowtan, K., Dodson, E., Evans, P. R., Jenkins, H. T., Keegan, R., Krissinel, E., & Stevenson, K. (2018). CCP4i2: the new graphical user interface to the CCP4 program suite. *Acta Crystallographica Section D: Structural Biology*, *74*(2), 68-84.

Powell, H. R., Battye, T. G. G., Kontogiannis, L., Johnson, O., & Leslie, A. G. (2017). Integrating macromolecular X-ray diffraction data with the graphical user interface iMosflm. *Nature protocols*, *12*(7), 1310-1325.

Sabarinathan, R., Mularoni, L., Deu-Pons, J., Gonzalez-Perez, A., & López-Bigas, N. (2016). Nucleotide excision repair is impaired by binding of transcription factors to DNA. *Nature*, *532*(7598), 264-267.

Sharma, V. K., Johnson, N., Cizmas, L., McDonald, T. J., & Kim, H. (2016). A review of the influence of treatment strategies on antibiotic resistant bacteria and antibiotic resistance genes. *Chemosphere*, *150*, 702-714.

Sherman, D. J., Lazarus, M. B., Murphy, L., Liu, C., Walker, S., Ruiz, N., & Kahne, D. (2014). Decoupling catalytic activity from biological function of the ATPase that powers lipopolysaccharide transport. *Proceedings of the National Academy of Sciences*, *111*(13), 4982-4987.

Simpson, B. W., Pahil, K. S., Owens, T. W., Lundstedt, E. A., Davis, R. M., Kahne, D., & Ruiz, N. (2019). Combining mutations that inhibit two distinct steps of the ATP hydrolysis cycle restores wild-type function in the lipopolysaccharide transporter and shows that ATP binding triggers transport. *MBio*, *10*(4), e01931-01919.

Stefan, E., Hofmann, S., & Tampé, R. (2020). A single power stroke by ATP binding drives substrate translocation in a heterodimeric ABC transporter. *Elife*, *9*, e55943.

Tan, L. T.-H., Chan, K.-G., Lee, L.-H., & Goh, B.-H. (2016). Streptomyces bacteria as potential probiotics in aquaculture. *Frontiers in microbiology*, *7*, 79.

Truglio, J. J., Croteau, D. L., Van Houten, B., & Kisker, C. (2006). Prokaryotic nucleotide excision repair: the UvrABC system. *Chemical reviews*, *106*(2), 233-252.

Van der Meij, A., Worsley, S. F., Hutchings, M. I., & van Wezel, G. P. (2017). Chemical ecology of antibiotic production by actinomycetes. *FEMS microbiology reviews*, *41*(3), 392-416.

Van Dyke, M. M., & Dervan, P. B. (1984). Echinomycin binding sites on DNA. *science*, *225*(4667), 1122-1127.

Wang, C.-H., Hsieh, Y.-H., Powers, Z. M., & Kao, C.-Y. (2020). Defeating antibiotic-resistant bacteria: exploring alternative therapies for a post-antibiotic era. *International journal of molecular sciences*, *21*(3), 1061.

Watanabe, K., Hotta, K., Praseuth, A. P., Koketsu, K., Migita, A., Boddy, C. N., Wang, C. C., Oguri, H., & Oikawa, H. (2006). Total biosynthesis of antitumor nonribosomal peptides in Escherichia coli. *Nature chemical biology*, *2*(8), 423-428.

Zhu, J., Chen, W., Li, Y.-Y., Deng, J.-J., Zhu, D.-Y., Duan, J., Liu, Y., Shi, G.-Y., Xie, C., & Wang, H.-X. (2014). Identification and catalytic characterization of a nonribosomal peptide

synthetase-like (NRPS-like) enzyme involved in the biosynthesis of echosides from Streptomyces sp. LZ35. *Gene*, *546*(2), 352-358.

Curriculum Vita

Gileydis Guillama Barroso is a United States permanent resident currently pursuing an M.S. degree in the Department of Chemistry and Biochemistry at The University of Texas at El Paso. She holds a B.A. in Chemistry from the University of Havana, Cuba, obtained in 2018. With a GPA of 4.00/4.00 in her current program and 4.07/5.00 in her undergraduate studies, Gileydis has demonstrated academic excellence. Her research interests lie in the field of chemistry and biochemistry. Gileydis has gained valuable experience in the academic and research sectors, having worked as a teaching assistant at The University of Texas at El Paso and as a research technician in the same department from 2019 to 2022. Prior to that, she worked as a researcher in the Department of Analytical Chemistry at the Petroleum Investigation Center in Cuba from 2018 to 2019. Gileydis has contributed to scientific literature with publications, including a research article and several review articles on topics such as environmental contamination and nanomaterial-based drug delivery systems. She has also mentored undergraduate students and presented her research findings at various scientific conferences and events.